IOP Publishing | Astro Ltd
Laser Physics Letters
Laser Phys. Lett. **15** (2018) 125101 (6pp)
https://doi.org/10.1088/1612-202X/aae21c

Letter

Properties of artificial saturable absorbers based on NALM with two pumped active fibres

Alexey Kokhanovskiy, Sergey Kobtsev, Aleksey Ivanenko and Sergey Smirnov

Division of Laser Physics and Innovative Technologies, Novosibirsk State University, Pirogova str., 2, Novosibirsk, 630090, Russia

E-mail: alexey.kokhanovskiy@gmail.com

Received 29 June 2018, revised 26 August 2018
Accepted for publication 11 September 2018
Published 5 October 2018

Abstract

This work reports for the first time the study of an artificial saturable absorber based on a non-linear amplifying loop mirror (NALM2) with two independently pumped active media instead of one (NALM). It is demonstrated that an adjustment of the ratio of the pump source power levels leads to a variation of the saturable power of an NALM2-based artificial saturable absorber within relatively broad limits. The transmission dependence of NALM2 upon peak power and variation of its shape as a function of the ratio of pump source power levels are established. The dynamics of the duration and shape of picosecond pulses at radiation peak powers close to the saturation power of NALM2 is also studied. It is shown that proper adjustment of the ratio of pump source power levels allows the maximal NALM2 saturation power to be shifted into a higher peak power of radiation pulses. The identified properties of NALM2 make it a universal saturable absorber for mode locking in fibre lasers with a variable peak pulse of ultra-short output pulses.

Keywords: nonlinear optical devices, optical properties, mode-locked lasers, nonlinear optics, pulse propagation and temporal solitons

(Some figures may appear in colour only in the online journal)

1. Introduction

So-called artificial saturable absorbers (ASAs) based on optical fibre whose non-linear properties may lead to intensity-dependent transmission are widely employed for mode locking in fibre lasers [1, 2] because they are free from the issues plaguing natural (non-artificial) saturable absorbers; namely, limited radiation power handling, a narrow working spectral range, performance degradation over time, etc [3–5]. Furthermore, slow relaxation times typical of natural absorbers lead to a deterioration in mode locking quality [4, 6]. Non-linear amplifying loop mirrors (NALMs) are especially important among ASAs used in fibre lasers [7–9] owing to a convenient way of NALM parameter adjustment by varying its pumping power. Nonetheless, the possibilities of this adjustment are limited; although it is possible to tune the duration and spectral width of the output pulses, their peak power remains constant [10–14]. In our earlier work [15], we showed that an NALM featuring two independently pumped active media instead of one makes it possible to also vary the peak pulse power in mode-locked operation. The new generation properties of lasers with such NALM have sparked interest in the exploration of this ASA, specifically as an individual optical element.

The present work is focused on the detailed study of NALM containing two independently pumped active media instead of just one (we will henceforth refer to it as NALM2).

The addition of a second active medium (or another amplifier) to NALM leads to a qualitative change in its nonlinear properties; essentially this creates a next-generation loop mirror. In [15], we explored the properties of a passively mode-locked fibre laser based on NALM2, whereas here we will analyse, experimentally and theoretically, the properties of NALM2 as an independent optical element, including the evolution of the duration and shape of picosecond pulses making a single pass across this element. The new properties of NALM2 we have identified provide a physical basis for understanding the peculiarities and advantages of mode locking in fibre lasers with the nonlinear amplifying loop mirrors of the new generation.

2. Experiment

The experimental set-up used to examine the NALM2 properties is schematically presented in figure 1.

Only polarisation-maintaining fibre-optical components were used in the studied NALM2 (to minimise the effect of non-linear polarisation evolution [11]). Two 2 m segments of ytterbium-doped gain fibre (YDF1 and YDF2) were pumped through their corresponding double-clad combiners by multimode laser diodes LD1 and LD2 delivering up to 9 W at 978 nm. The gain segments YDF1 and YDF2 were connected with 10 m of passive fibre. Radiation input/output was carried through a 50/50 coupler connected to YDF1 and YDF2 with 0.2 m long pieces of passive fibre. Depending on the nonlinear phase difference of the waves passing through NALM2 in opposite directions (the input wave is divided into two counter-propagating ones by the 50/50 coupler), the output radiation may also propagate in two directions: into the output port (transmission port in figure 1) and into the input port (reflection port in figure 1). To measure the radiation parameters at the exit from ports T and R, we used a laser power meter and a scanned auto-correlator FS–PS–auto with a working pulse duration range of 10 fs–35 ps.

Input pulses were provided by a mode-locked NPE-based all-positive-dispersion all-fibre Yb master oscillator connected to a fibre optical amplifier. The energy of the pulses fed into NALM2 was tuned by adjusting the gain in the fibre amplifier (through variation of the amplifier pump source power). In this way, it was possible to set the peak power of the input NALM2 pulses up to 140 W, while keeping the spectral width and the temporal envelope of the input pulses at different energy levels. Figure 2 demonstrates the radiation spectrum and the temporal profile of the used input pulses. It can be seen in figure 2 that the input pulse spectrum is approximately 11 nm wide and has a complicated shape, which is not optimal for the experimental studies of spectral transformations of pulses in NALM2. Consequently, in our experiment, we limited ourselves to measurements of energy and temporal parameters of the pulses exiting NALM2, while in our numerical modelling, we considered NALM2 conversion of pulses with different spectral widths: 0.18 nm wide (spectrally limited pulses), 10 nm wide (chirped pulses close to the experimental ones), and 20 nm wide (pulses with even higher chirp).

The input pulse duration amounted to 10.4 ps at a repetition frequency of 20.5 MHz. The duration of around 10 ps was selected because pulses with similar duration are generated in a laser with NALM2 [15]. For ease of comparison between the transmission curves of NALM2 at different pump power levels, we used an NALM2 transmission coefficient T normalised to NALM2 gain coefficient g:

$$T = P_T/(g \cdot P_{IN}) = P_T/(P_T + P_R), \quad (1)$$

where P_{IN} is the power of input pulses, P_T is the power of transmitted pulses, P_R is the power of reflected pulses, and g is the gain of NALM2 that is equal to $(P_R + P_T)/P_{IN}$.

Figure 3(a) shows the dependence of this normalised NALM2 transmission upon the peak power of the input pulses at different power levels of the YDF2 pump (1, 2.3, 3.5 W) and fixed power of the YDF1 pump (3.7 W). The power levels of the pump sources were intentionally kept different because at equal gain in active media YDF1 and YDF2, the input radiation is entirely coupled back into port R (that is, totally reflected from NALM2). The transmission curve corresponding to 1 W of pump power of YDF2 has an oscillating behaviour and has an absolute maximum at relatively low values of the input peak power, which we will refer to below as the first transmission maximum. Figure 3(a) also demonstrates a shift of this maximum towards higher peak input power values at higher YDF2 pump levels making it possible to reach the highest saturation power of NALM2 for higher input peak powers.

It is interesting to compare the transformation of the transmission curves characterising NALM2 and the traditional NALM at different peak powers of the input pulses. To perform such a comparison, active fibre YDF1 was removed from the studied NALM2 and then the dependence of the NALM transmission upon the input peak power was measured for the same values of the YDF2 pump power. The results of this measurement are shown in figures 3(a) and (b) where transmission curves corresponding to NALM2 and NALM exhibit radically different dynamics. As the total gain in the fibre loop is raised, the NALM2 transmission maxima are shifted towards higher peak pulse powers, whereas NALM transmission maxima present the opposite dynamics and are thus shifted towards lower peak pulse powers. Therefore, the addition of a second active medium (or another amplifier) to a nonlinear amplifying loop mirror may lead to its transmission maximum of a given order (first, second, ...) corresponding to a higher peak pulse power. It is this specific property combined with an ultra-long cavity that has made it possible to achieve record-setting pulse energies in a mode-locked fibre master oscillator with NALM2 [16]. Notwithstanding the similarities in the transmission functions of NALM and NALM2, their dynamics contrast when the pump level is raised (one of the two pumps for NALM2). This difference underpins the novelty and distinction of NALM2 compared to NALM.

The curve of figure 3(a) corresponding to NALM2 transmission at YDF2 fibre pumped with 1 W (blue squares) has two maxima: the first at an input peak power of 10 W and the second at around 130 W. A natural question arises as to whether NALM2 is able to ensure stable generation at higher-order maxima, second, third, etc. In order to determine this, we performed numerical modelling of the evolution of a

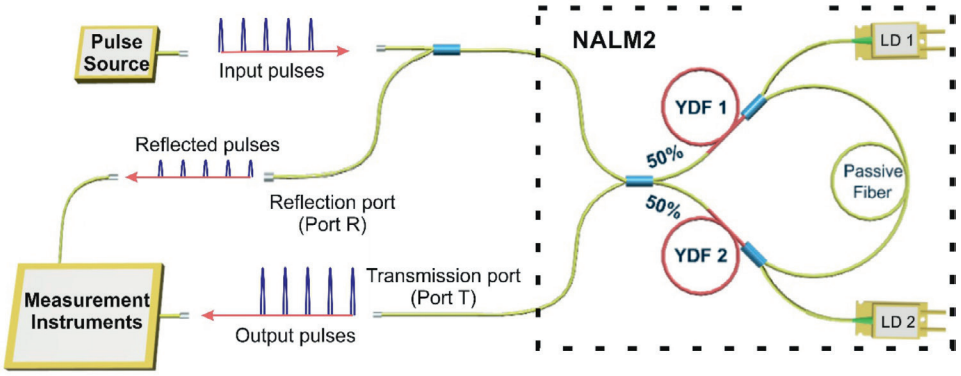

Figure 1. Experimetal set-up for the study of NALM2 properties.

picosecond pulse passing through NALM2 at different values of the input peak power.

3. Numerical modeling

To simulate the properties of NALM2, we used a numerical model based on the non-linear Schrodinger equation [17]:

$$\pm\frac{\partial A}{\partial z} = i\gamma|A|^2A - \frac{i}{2}\beta_2\frac{\partial^2 A}{\partial t^2} + \frac{Ag_0/2}{1+E/E_{sat}}, \qquad (2)$$

where $\pm$ corresponds to the forward and backward counter-propagating waves, $A(z;t)$ is the optical field envelope, z stands for the longitudinal coordinate along the fiber, t is time in the retarded frame of reference, γ and β_2 are non-linear and dispersion coefficients correspondingly, g_0 and E_{sat} stand for unsaturated gain coefficient and saturation energy for the active fibre, and $E = E_+ + E_- = \int|A_+|^2dt + \int|A_-|^2dt$ is the total energy of the counter-propagating waves. Equating g_0 to zero, this model can be used to calculate the propagation of the optical wave in a passive fibre. The fibre lengths and the coupler ratio of the numerical model correspond to those of the experimental set-up. The chromatic dispersion and non-linear coefficient of the polarization-maintaining fibre were equal to $\beta_2 = 2.3\cdot10^{-28}\frac{s^2}{m}$, $\gamma = 4.7\cdot10^{-3}\frac{1}{m\cdot W}$.

Let us note that laser pulses travel within the NALM in both directions and that both waves saturate the active fibers. Thus, equation (2) is in fact a system of two coupled equations for counterpropagating waves, which is solved in two stages during each cavity round-trip simulation [15]. In the first stage, self-consistent energy distributions $E_\pm(z)$ of counterpropagating waves are evaluated according to equation (3), which can be derived from equation (2):

$$\frac{E_\pm}{dz} = \pm\frac{g_0\cdot E_\pm}{1+E/E_{sat}}. \qquad (3)$$

Once $E_+(z)$ and $E_-(z)$ are known, at the second stage we can integrate equation (2) independently for A_- and A_+ using the well-known split-step Fourier method [17].

Higher pump levels of active fibre in the experiment correspond to the higher saturation energy E_{sat} of the numerical model. E_{sat} will be varied across the study for simulating different pump power levels—particular values will be indicated

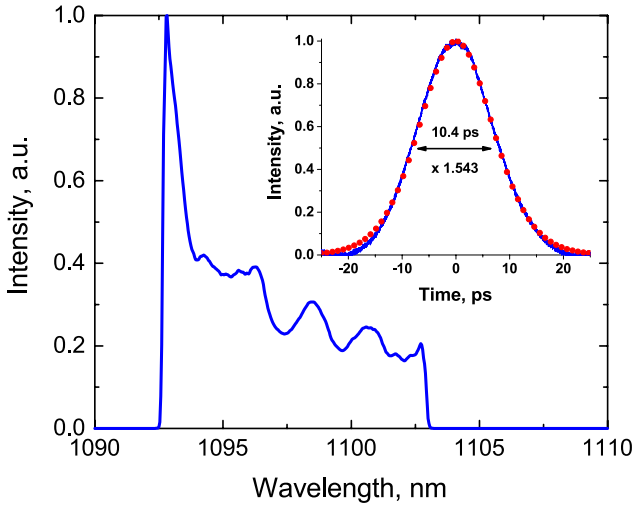

Figure 2. Input pulse spectrum. Inset: auto-correlation function of the input pulses.

in the text. Shown in figure 4 are the calculated NALM2 transmission curves at the input pulse duration of 10 ps and spectral width of 0.18 and 10 nm.

It is evident that the general shape of the curve practically does not depend on the spectral width of the input pulses, whereas the loci of the NALM2 transmission maxima depend on the spectral width and this dependence steepens at higher transmission peak numbers: the position of the first transmission peak is relatively weakly affected by the spectral width of the input pulses, but the second peak position is shifted further, and so forth.

We tested input pulses at a wavelength of 1.09 μm with a fixed 10-ps duration and different spectral widths: transform-limited pulses with a spectral width of 0.18 nm and linearly chirped pulses with a 10 nm spectral width that are closed to the experimental one. We were interested in tranform-limited pulses with a narrow specral width because such pulses are typical for mode-locked lasers with NALM and without additional spectral filtration of radiation [16, 18, 19]. Given in figure 4 is the calculated transmission dependence of NALM2 upon the peak power of input pulses. It is in qualitative agreement with the measured experimental data of figure 3.

The chosen numerical model also tracked the pulse shape transformation upon passing through NALM2. Figure 5 shows

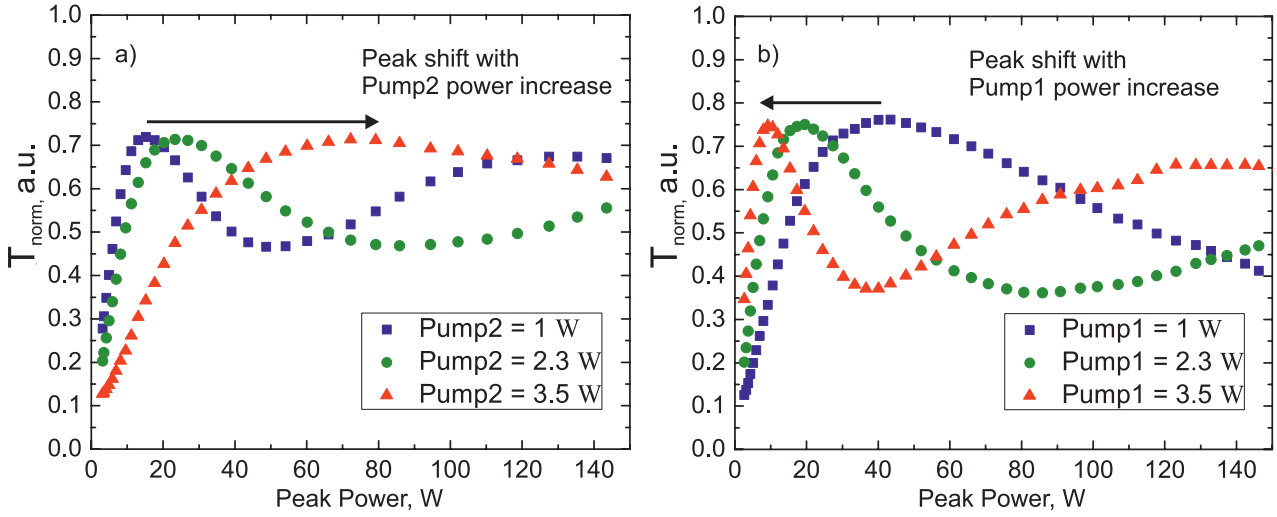

Figure 3. (a) Dependence of NALM2 transmission (normalised) upon input peak power at different levels of YDF2 pump power and a fixed pump power of YDF1. (b) Dependence of NALM transmission (normalised) upon input peak power at different levels of pump power launched into the NALM active fibre.

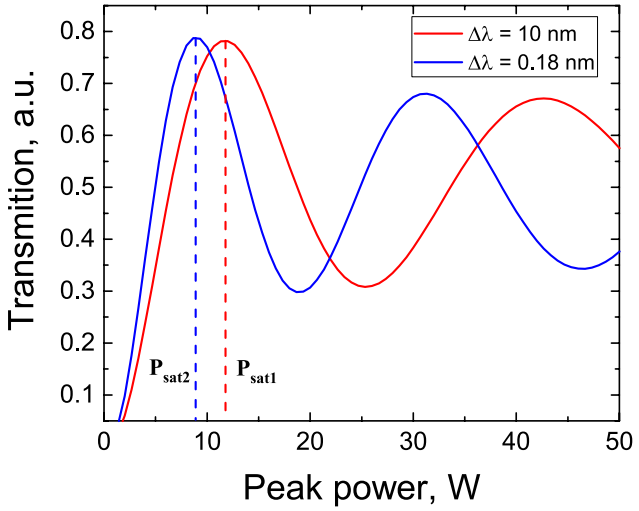

Figure 4. Dependence of NALM2 transmission (normalised) upon the peak power of the input pulse. $g_0 = \frac{1}{\text{cm}} E_{sat1} = 15$ nJ, $E_{sat2} = 2$ nJ for pulses with different spectral widths.

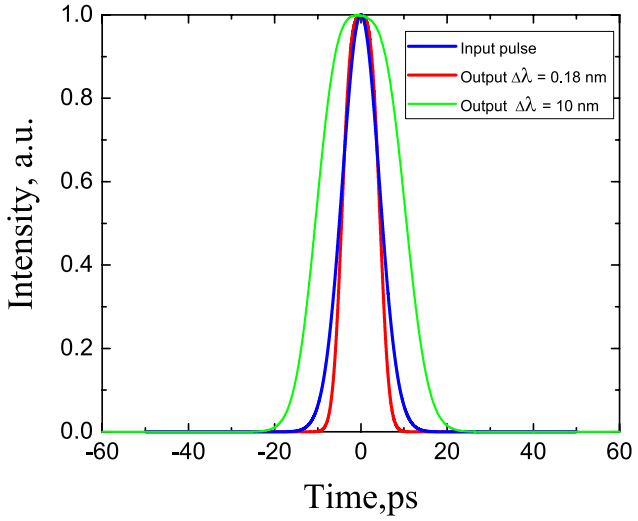

Figure 5. Temporal intensity distributions of the input and output pulses at different spectral widths of the input pulses.

the temporal intensity distribution of both input and output pulses at the input peak power of 8.3 W that corresponds to the saturation power of NALM2 for a transform-limited pulse or the first maximum of the normalized transmission curve. It can be seen that the output pulse top is flattened when NALM2 is saturated compared to the input pulse with a 0.18 nm spectral width. Similar 'squaring' of the temporal envelope of the NALM2 output pulses is observed at the input pulse spectral width of 10 nm. In this case, however, the output pulse duration is twice that of the input pulses, which is an effect of the chromatic dispersion of chirped pulses in NALM2.

When analysing the input pulse temporal profile transformation during a single pass through NALM2, we were first of all interested in conditions leading to low deformation. In our opinion, such conditions are a pre-requisite for stable stationary 'single-pulse' mode locking (with a single pulse circulating around the cavity). The conditions (active media gain, peak input power) leading to the development of additional pulses in the temporal intensity distribution upon a single pass through NALM2 do not correspond to stable stationary 'single-pulse' mode locking, since amplification of such additional pulses over the subsequent passes through NALM2 may lead to a multi-pulse transient generation regime with no or only partial mode locking [20]. In figure 6, we show a modelled evolution of temporal and spectral intensity distributions within the NALM2 output pulses dependent on the peak power of the input pulses with a spectral width of 10 nm (figure 6(a)) and 0.18 nm (figure 6(b)).

The salient feature of the distributions in figure 6 is decomposition of the pulse in both temporal and spectral representation into two and more components when the input pulse peak power exceeds a certain threshold value P_{sat} (dashed line in figure 6). From this it follows that a self-reproducing pulse generation regime in NALM2 is only possible at an input pulse peak power below P_{sat}. However, NALM2 makes it possible to shift the value of P_{sat} into higher peak powers of the input pulses due to an increase in the power of one of the two

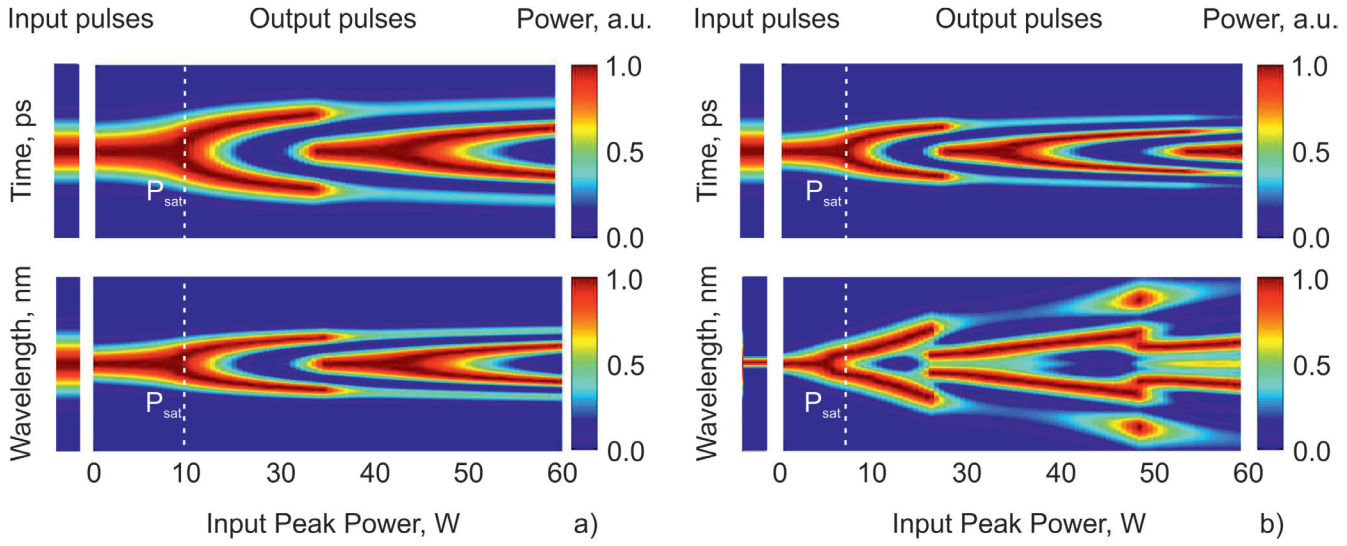

Figure 6. Temporal distributions of the NALM2 output pulse as a function of the input pulse peak power: (a) chirped pulses with 10 nm spectral width, (b) transform-limited pulses with 0.18 spectral width. The colour code corresponds to the pulse peak power normalised to its maximum power. The color bar corresponds to a peak power of the pulse normalised by its maximum power.

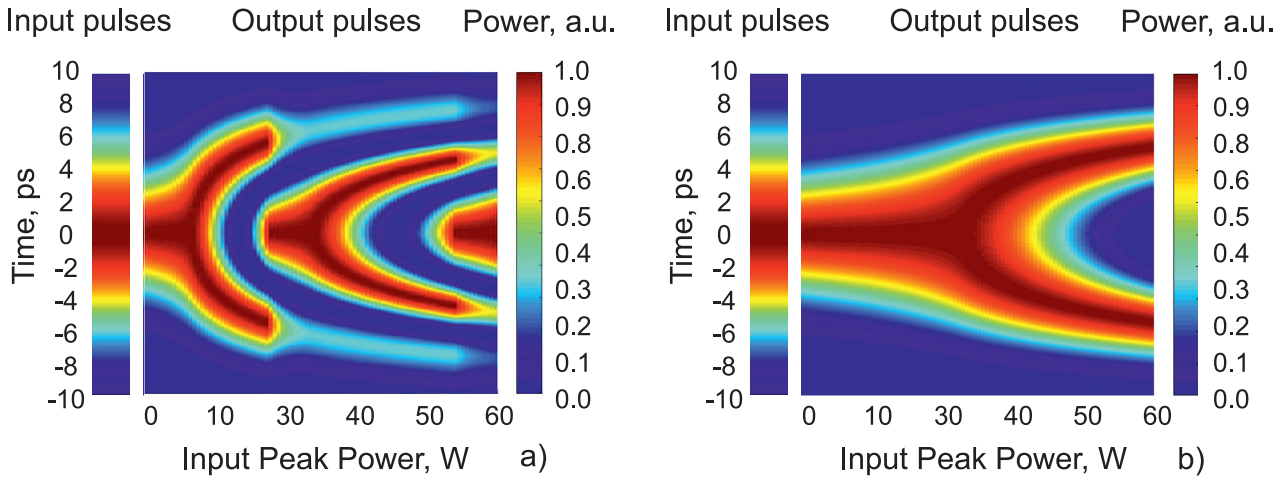

Figure 7. Temporal distributions of the NALM2 output pulse as a function of the input pulse peak power: (a) $g_0 = 1\frac{1}{\text{cm}}, E_{sat1} = 15$ nJ, $E_{sat2} = 2$ nJ (b) $g_0 = 1\frac{1}{\text{cm}}, E_{sat1} = 15$ nJ, $E_{sat2} = 8$ nJ. The color bar corresponds to a peak power of the pulse normalised by its maximum power.

pump sources, as shown in figure 7. It can be seen that the low-deformation domain was stretched up to 30 W, indicating that higher gain in NALM2 effectively leads to a higher peak power of pulses experiencing minimal deformation of their temporal shape when passing through NALM2.

One of the key features of NALM2 is its ability to temporally compress pulses at a relatively low peak power. In the single-pass mode, the pulse duration may be reduced by as much as 10%, which may lead, along with a similar amount of pulse dispersion broadening over the rest of the laser cavity, to stationary mode locking. According to our modelling, the ratio of the input and output duration of the pulse processed by NALM2 largely depends on the pulse spectral width. In order to estimate the possible range of this ratio, we considered its dependence for pulses with different spectral widths at different saturation powers of active fibre YDF2 and at a fixed saturation power active fibre of active fibre YDF1. Figure 8 presents the modelling results for Gaussian pulses with different spectral widths of 0.18 nm (red curve), 10 nm (green curve), and 20 nm (blue curve). The last two were implemented by stretching a transform-limited Gaussian pulse in a length of dispersive fibre. Overall, it is obvious that at a given spectral width, the ratio of the input and output pulse duration has no marked dependence upon the pump level of active fibre YDF2. A relatively narrow pulse spectrum (0.18 nm in our case), when dispersion may be ignored (characteristic dispersion length much larger than the NALM2 length: $L_D \gg L_{\text{NALM2}}$), corresponds to the coefficient of the temporal compression of a picosecond pulse passing through NALM2 in the vicinity of 0.9. Therefore, for picosecond pulses with a relatively narrow spectrum, NALM2 plays the role of a temporal compressor, and application of NALM2 in mode-locked lasers without special spectral filtration may lead to the generation of pulses with a narrow optical spectrum. For input pulses with a relatively broad spectrum, when the characteristic dispersion length is much shorter than that of NALM2

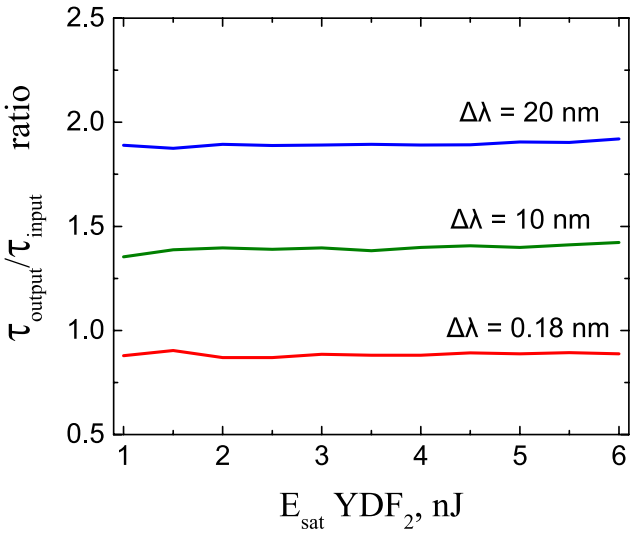

Figure 8. Duration ratio of NALM2 input and output pulses as a function of the pump power of active fibre YDF2 at different values of the pulse spectral width.

($L_D \ll L_{NALM2}$), the effect of the dispersion broadening of pulses in NALM2 dominates, and, as our modelling shows, may lead to several-fold pulse stretching over a single pass through NALM2. In this case, the temporal stretching of the input pulses with a given spectrum will be governed by the NALM2 length.

4. Conclusion

The key properties of an ASA based on NALM2 were studied both experimentally and theoretically. It was discovered that NALM2 differs fundamentally from conventional NALM in that higher gain in the latter shifts its transmission maxima towards lower peak power values of input pulses, whereas NALM2 transmission maxima are shifted in the opposite direction towards higher peak powers. This allows NALM2 saturation at a higher peak power of radiation pulses. Specifics of pulse shape evolution in NALM2 were identified, which make it preferable to use NALM2 around its first transmission maximum. We also established conditions of pulse temporal compression in NALM2 and found an effect of pulse top flattening after passing through NALM2. The presented, newly discovered properties of NALM2 make it an attractive component for mode-locked fibre lasers with a high and variable peak power of output pulses. The only disadvantage of NALM2 is its higher cost because of an additional amplifier as compared to conventional NALM. However, NALM2 provides significant additional flexibility and enables the generation of record-high pulse energy directly in a mode-locked fibre master oscillator. An important advantage of the proposed NALM2 solution is the possibility and relative simplicity of electronic control over pump power levels, essentially by adjustment of the injection current of the pumping laser diodes. Such a solution corresponds, in general, to the fibre laser concept, which does not include any manual controls and implies only electronically controlled adjustments. Practical implementation of NALM2 is not complicated because it is based on standard fibre components. Moreover, NALM2 may be created by upgrading an existing conventional NALM.

Acknowledgments

Work was supported by the Russian Science Foundation (17-12-01281).

References

[1] Fermann M E and Hartl I 2013 *Nat. Photon.* **7** 868
[2] Du Y, Shu X and Xu Z 2016 *Opt. Lett.* **41** 360–3
[3] Ryu S Y, Kim K S, Kim J and Kim S 2012 *Opt. Express* **20** 12966–74
[4] Viskontas K, Regelskis K and Rusteika N 2014 *Lithuanian J. Phys.* **54** 127–35
[5] Kobtsev S, Ivanenko A, Gladush Y G, Nyushkov B, Kokhanovskiy A, Anisimov A S and Nasibulin A G 2016 *Opt. Express* **24** 28768–73
[6] Kuse N, Jiang J, Lee C C, Schibli T and Fermann M 2016 *Opt. Express* **24** 3095–102
[7] Duling I, Chen C J, Wai P and Menyuk C 1994 *IEEE J. Quantum Electron.* **30** 194–9
[8] Aguergaray C, Hawker R, Runge A F, Erkintalo M and Broderick N G 2013 *Appl. Phys. Lett.* **103** 121111
[9] Hänsel W *et al* 2018 *Exploring the World with the Laser* (Berlin: Springer) pp 331–40
[10] Avdokhin A, Popov S V and Taylor J 2003 *Opt. Express* **11** 265–9
[11] Ding E, Grelu P and Kutz J N 2011 *Opt. Lett.* **36** 1146–8
[12] Yang J H, Guo C Y, Ruan S C, Ouyang D Q, Lin H Q, Wu Y M and Wen R H 2013 *IEEE Photonics J.* **5** 1500806
[13] Lin H, Guo C, Ruan S and Yang J 2014 *Laser Phys. Lett.* **11** 085102
[14] Grelu P and Akhmediev N 2012 *Nat. Photon.* **6** 84
[15] Smirnov S, Kobtsev S, Ivanenko A, Kokhanovskiy A, Kemmer A and Gervaziev M 2017 *Opt. Lett.* **42** 1732–5
[16] Ivanenko A, Kobtsev S, Smirnov S and Kemmer A 2016 *Opt. Express* **24** 6650–5
[17] Agrawal G P 2000 *Nonlinear Science at the Dawn of the 21st Century* (Berlin: Springer) pp 195–211
[18] Li X *et al* 2011 *Laser Phys.* **21** 940–4
[19] Li D, Li L, Zhou J, Zhao L, Tang D and Shen D 2016 *Sci. Rep.* **6** 23631
[20] Churkin D, Sugavanam S, Tarasov N, Khorev S, Smirnov S V, Kobtsev S M and Turitsyn S K 2015 *Nat. Commun.* **6** 7004